2025 23rd European Control Conference (ECC)
June 24-27, 2025. Thessaloniki, Greece

Degradation-Conscious Model Predictive Control For Marine Solid-Oxide Fuel Cells

Andrea Caspani, Rudy R. Negenborn and Vasso Reppa

Abstract— **Solid Oxide Fuel Cells (SOFCs) represent a promising technology in the field of electric power generation, particularly suited for alternative fuels and large-scale applications. With the marine industry targeting a full decarbonization by year 2050, there is a significant effort towards the adoption of SOFCs in cargo ships and other vessels. However, their effective adoption in marine transportation requires improved reliability, especially regarding cell degradation, which directly affects their functional lifetime. This paper proposes a novel Degradation-Conscious control strategy for SOFCs, integrating direct control of cell voltage degradation. First, we propose a novel state space model comprising a reduced order model of SOFC dynamics and the voltage degradation model of the cell. Second, we develop the Degradation-Conscious controller using a nonlinear Model Predictive Controller, which integrates degradation management into standard SOFC dynamical control. Simulation results demonstrate the proposed strategy's ability to reduce degradation while meeting dynamical performance requirements.**

I. Introduction

In 2018, the maritime industry accounted for 2.89% of global Greenhouse Gas emissions. In recent years, the International Maritime Organization (IMO) set 2050 as target year for a complete decarbonization of the sector, effectively stressing the development of robust and reliable alternative power generation systems. In this context, Solid Oxide Fuel Cells (SOFCs) stand out as a promising technology to limit carbon emissions in large-scale maritime applications, thanks to their energy efficiency and ability to use alternative fuels including hydrogen, ammonia, and methanol.

Despite the benefits, a number of improvements in system performance and reliability are still needed before SOFCs can be widely used as energy converters for maritime applications, regardless of the utilized fuel. The primary disadvantages include limited dynamic performance, cell deterioration, and an overall increased system complexity [1]. A common factor contributing to these issues is the cell operation: an improper operation can easily damage the SOFC system and subsystems, and reduce their lifespan. SOFC voltage degradation, in particular, is closely related to system operating conditions, including cell temperature, current demand, and fuel and air utilization, among others. Recent studies evaluating the long-term durability of SOFCs report voltage degradation rates ranging from 0.5% to 1.4% per 1,000 hours of operation in steady state [2]. Moreover, the dynamic nature of marine operations and operating conditions, creates additional stress on SOFC systems.

In addressing these challenges, the development of SOFC tailored control strategies becomes essential. Traditionally, SOFC control relies on the management of inlet flows (i.e., air and fuel) and of the required current, to ensure stable temperature control, while maintaining robust electrical output and efficient electrical load following. In the current state of practice, this is mostly done by means of Proportional-Integral-Derivative (PID) controllers, as discussed in [3] and in [4]. However, despite their simplicity and ease of implementation, PID controllers often lead to sub-optimal performances (e.g., *PID cannot meet the current control requirements because of the increased demand for accuracy* [5]). To overcome these limitations several alternative control strategies have been investigated so far. Model based control strategies such MPC showed satisfactory performance, like in [6], by utilizing a dynamic process model for predictive optimization, enhancing robustness and stability while effectively managing the constraints. Similarly, data-driven methods, such as the reinforcement learning algorithm proposed in [7], demonstrated improved control performance and robustness, while maintaining appropriate input management.

In parallel, several methods have been developed to track SOFCs faulty working conditions, and their performance degradation over time. The authors in [8] proposed a Fault Detection and Isolation (FDI) oriented modelling of an experimental SOFC system, accounting for different classes of faults such as leakages, and reformer degradation. In [9] instead, the authors provide a reliable estimate of the Remaining Useful Life (RUL) of a SOFC system based on cell's areas specific resistance (ASR) drift. Thus, linking a physical detrimental state of a cell component to a health indicator of the overall system. However, these approaches typically focus on assessing the health status of the SOFC, while this information is not exploited to adapt the cell operation and to mitigate the degradation effects. However, in Safety-critical operations it is essential not only to monitor SOFC health indicators (i.e., track system deterioration), but also actively manage and optimize the system operating condition to balance between real time performance and the mitigation of long term degradation effects.

In control theory, integrating the system health status into the control strategy is referred to as Health-Aware Control (HAC). The main concept behind these methods is to *take into account the system's health information in the control objectives. In this way, the control actions*

Department of Maritime and Transport Technology, Faculty of Mechanical Engineering, Delft University of Technology, Mekelweg 2, 2628 CD Delft, the Netherlands. (e-mail: a.caspani@tudelft.nl, v.reppa@tudelft.nl, r.r.negenborn@tudelft.nl)

This research has been performed as part of the project AmmoniaDrive, funded by the NWO Perspectief Programme under Grant no. P20-18/14267.

are generated to fulfill the control goals and, at the same time, to extend the life of the system components, [10]. HAC incorporates broader health metrics (e.g., operational efficiency, reliability, and degradation rate, among others), RUL, and fault-tolerant behavior, allowing the controller to dynamically adjust based on the system's overall health state, thus balancing performance and reliability. A similar technique is the so called Degradation-Conscious Control (DCC), see [11], which focuses specifically on incorporating known or modeled information about the degradation of the controlled dynamical system into the control loop. DCC aims to minimize the effects of degradation over time, adjusting control actions to slow down the degradation process, often at the cost of short-term dynamical performance, as it as it has to balance multiple (and possibly opposing) objectives.

Contribution

This paper proposes a Degradation-Conscious Nonlinear Model Predictive Control (DC-nMPC) strategy specifically designed for marine SOFCs, focusing on balancing dynamic performance and long-term degradation management. The key contributions are summarized as follows:

1. Integration of an SOFC reduced order model (SOFC-ROM) with a cell voltage degradation model combining the SOFC-ROM dynamics from [12] with the voltage degradation model derived in [13].

2. Development of the DCC-nMPC controller: We design a Degradation-Conscious Controller, inserted in a nonlinear Model Predictive Control framework, to address SOFC nonlinearity while balancing between dynamic performance, characterized by load following and temperature regulation, and overall limitation of cell voltage degradation.

Simulation results show the capability of this method to meet standard SOFC dynamical performance while limiting its overall voltage degradation through time. Thus extending SOFC lifespan and making this technology promising for their effective adoption in the marine industry.

II. System Modelling

In the following section, we present the SOFC dynamical and degradation models, first in their physical formulation, and later in state space. SOFC system are also referred to as *stacks*, composed by multiple *cells*, which are the individual electrochemical units that convert fuel into electricity. In our work we focus on a stack composed by a single cell, therefore we will refer to the SOFC also as the *cell*.

Fig. 1 depicts a simplified scheme of a SOFC stack, highlighting the cells, the physical quantities of interest.

A. Physical model of cell dynamics

The dynamical model of the cell employed in this work is the one introduced in [12] and [14]. It is a reduced order model of solid oxide fuel cell (SOFC-ROM). This formulation is zero-dimensional, meaning that it assumes a constant temperature T throughout the entire cell and it is parametrized on an existing methane fueled SOFC.

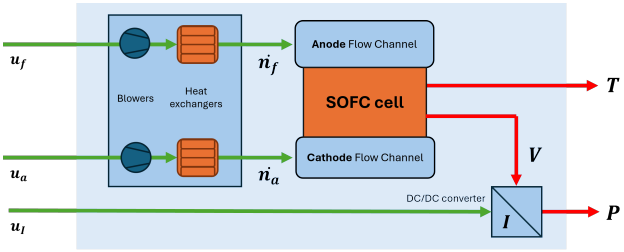

Fig. 1. Simplified scheme of a generic stand-alone SOFC system

At the anode of the cell, a preheated mixture of gases is supplied as fuel, composed of the following chemical species: methane (CH_4), carbon dioxide (CO_2), carbon monoxide (CO), water vapor (H_2O), and hydrogen (H_2). At the cathode, preheated air is supplied, composed of oxygen (O_2) and nitrogen (N_2). The main chemical reactions considered to occur inside the cell are methane steam reforming (MSR), the water-gas shift reaction (WGS), and the hydrogen oxidation reaction (HOR).

Before introducing the model, we clarify the notation: the subscript $i \in \mathcal{S} := \{\mathrm{CH_4}, \mathrm{CO_2}, \mathrm{CO}, \mathrm{H_2O}, \mathrm{H_2}, \mathrm{O_2}, \mathrm{N_2}\}$ refers to an individual chemical species, such that X_i represents the property X of the species indexed by i. When referring to a specific species, the subscript is explicitly specified, e.g., $X_{\mathrm{CH_4}}$ represents the property X of methane (CH_4). The subscript $j \in \mathcal{F} := \{f, a\}$ designates the fuel f and air a streams, indicating that X_f represents the property X of the fuel stream, and X_a represents the property X of the air stream. The subscript $m \in \{\text{MSR, WGS, HOR}\}$ refers to a specific reaction, so that X_m represents the property X for reaction m. Finally, expressions with an overline (e.g., $\overline{X}$) denote constant values.

The dynamical equations are the following:

$$\frac{dT}{dt} = \Bigg(\underbrace{\sum_{\substack{i\in\mathcal{S},\\ j\in\mathcal{F}}} \left(n_j \overline{K}_i h_i(\overline{T}_i) - \left(n_j \overline{K}_i + \textstyle\sum_m \overline{\nu}_{i,m} r_m\right) h_i(T)\right)}_{\text{Enthalpy Balance}} - \underbrace{IV}_{\text{Electric Power}} - \underbrace{\overline{\lambda}(T - \overline{T}_a)}_{\text{Heat Losses}} \Bigg) \frac{1}{\overline{c}_p} \tag{1}$$

$$V = \underbrace{-\frac{\Delta g}{2\overline{F}} + \frac{\overline{R}T}{2\overline{F}} \ln(Q)}_{\text{Nernst voltage}} - \underbrace{\frac{IR_a}{\overline{A}}}_{\text{Ohmic losses}} \tag{2}$$

The differential equation in (1) consists of the following components:

Enthalpy Balance: The first term represents the net enthalpy flow rate entering and exiting the system. Here, T(K) denotes the internal temperature of the cell, while n_j(mol/s) represents the molar flow rates of the fuel (n_f) and

air (n_a) entering the system. The specific enthalpy of species i at temperature T is denoted by h_i(J/mol), and r_m(mol/s) denotes the reaction rate of reaction m. The constant $\overline{K}_i$(-) represents the concentration of species i within the molar flow n_j, $\overline{\nu}_{i,m}$(-) is the stoichiometric coefficient of species i in reaction m, while $\overline{T}_i$(K) is the constant inlet temperature of species i.

The specific enthalpy h_i is calculated using the Shomate equation, with coefficients obtained from the National Institute of Standards and Technology (NIST) Chemistry WebBook [15] [16]. The reaction rates r_m of the three reactions are the following: $r_{\text{MSR}} = n_{\text{CH}_4}$ assuming that all the methane is reformed within the cell, $r_{\text{HOR}} = \frac{I}{2\overline{F}}$, which is directly proportional to the cell current according to Faraday's law, while r_{WGS} has been computed using a symbolic solver as in [12].

2. **Electric Power**: The second term in (1) represents the electrical power generated by the electrochemical reactions. In this term, I(A) denotes the current, and V(V) is the cell voltage, as expressed in (2).

3. **Heat Losses**: The final term represents the heat losses and is calculated using Newton's cooling law, where $\overline{T}_a$ is assumed to be 25 ° C and $\overline{\lambda}$(J/s·K) is the heat transfer coefficient.

Equation (2) describes the cell voltage and it consists of the *Nernst Voltage* minus the *Ohmic losses* (in this ROM, various over-potential losses are simplified to a single, purely Ohmic loss). In this expression, Δg(J/mol) represents the Gibbs free energy of the HOR reaction at temperature T. Q(-) is the reaction quotient and is given by:

$$Q = \frac{(n_{\text{H}_2} + \sum_m \overline{\nu}_{\text{H}_2,m} r_m)(n_{\text{O}_2} + \sum_m \overline{\nu}_{\text{O}_2,m} r_m)^{\frac{1}{2}}}{n_{\text{H}_2\text{O}} + \sum_m \overline{\nu}_{\text{H}_2\text{O},m} r_m} \tag{3}$$

The second expression in (2) represent the Ohmic losses. Here, R_a, is the area specific resistance of the cell. Moreover $\overline{F}$(C/mol) is the Faraday constant, $\overline{R}$(J/mol·K) is the universal gas constant and $\overline{A}$(m²) is the active area of the electrode.

Last, we need to account for two physical constraints: fuel utilization and air utilization. Fuel utilization μ_f(-) represents the fraction of fuel that has been effectively converted into electrical power. Air utilization μ_a(-) indicates the fraction of oxygen used in the HOR. These factors are defined as follows:

$$\mu_f = \frac{I}{2\overline{F}\,(4n_{\text{CH}_4} + n_{\text{CO}} + n_{\text{H}_2})}, \quad 0 \le \mu_f \le 1 \tag{4}$$

$$\mu_a = \frac{I}{4\overline{F} n_{\text{O}_2}}, \quad 0 \le \mu_a \le 1 \tag{5}$$

μ_f, as an indicator of cell efficiency, is typically maintained above 0.6 to optimize performance [3].

B. Auxiliary Units Model

SOFCs are complex systems composed of a large number of components. In our formulation, we focus primarily on the cell itself, assuming that the other auxiliary components (e.g., fuel and air blowers, heat exchangers, DC-DC converter, etc.) operate as expected. To account for the fact that input management is not instantaneous, we incorporate these actuators dynamics by modeling low-pass filters for the three primary input variables: fuel flow n_f, air flow n_a, and current I. The filters are first-order, and their differential equation formulation is given by:

$$\dot{z}_j = -\frac{1}{\overline{\tau}_j} z_j + \frac{1}{\overline{\tau}_j} u_j \tag{6}$$

where $z_j = [n_f, n_a, I]$, is the input entering the physical system, $u_j = [u_f, u_a, u_I]$ is the control input and τ_j(s) is the associated time constant.

C. Voltage Degradation Model

The voltage degradation model is based on the experimental findings in [13]. It is important to note that this formulation specifically describes the rate of increase in the cell's area-specific resistance R_a(Ω·m²), which directly contributes to ohmic losses. While cell voltage is influenced by various factors, ohmic losses can account for up to 20% of total efficiency losses in electrochemical cells [17].

The voltage degradation of the cell is represented by a drift in the Area Specific Resistance R_a over time, which is given by the following differential equation:

$$\frac{dR_a}{dt} = \frac{\overline{k}_1 \mu_f + \overline{k}_2}{1 + e^{\frac{T - \overline{k}_3}{\overline{k}_4}}} \left(e^{\frac{\overline{k}_5 I}{\overline{A}}} - 1 \right) \frac{R_a}{\overline{k}_0} \tag{7}$$

This expression describes the rate of change of the area-specific resistance R_a as function of the operating condition of the cell, namely temperature T, current I and fuel utilization μ_f. Initially, R_a begins at a baseline value, representing a new, non-degraded cell. As time progresses, R_a increases whenever the cell operates under non-zero current. This cumulative effect models the aging process, capturing how prolonged usage, particularly at low temperatures, high currents, and high fuel utilization, leads to an increase in R_a and, consequently, a decline in cell efficiency. The constants $\overline{k}_0, \ldots, \overline{k}_5$ are empirical values derived from long-term experiments, as reported in [13].

D. SOFC Degradation-Conscious Operation

The objective of our work is to control the SOFC described by the physical models introduced in (1)-(7) in a Degradation-Conscious fashion. This is achieved through three main objectives: first, by ensuring electrical load following, second, by maintaining system temperature at a predefined operating point and third by minimizing the degradation rate in real-time.

III. Method

A. Degradation-aware State Space Model

The state space formulation we introduce below is based on the physical models introduced before.

The states are the differential variables T and R_a in (1) and in (7), and the inputs coming from the actuators as introduced in (6). The state vector x therefore defined as

$x = \begin{bmatrix} T & R_a & n_f & n_a & I \end{bmatrix} \in \mathbb{R}^5$, while the inputs vector is defined as $u = \begin{bmatrix} u_f & u_a & u_I \end{bmatrix} \in \mathbb{R}^3$.

Given this set of variables we can now define some functions that will be useful in the state space formulation:

$$f(x) = \sum_{\substack{i\in\mathcal{S},\\ j\in\mathcal{F}_x}} \left(x_j \overline{K}_i h_i(\overline{T}_i) - \left(x_j \overline{K}_i + \textstyle\sum_m \overline{\nu}_{i,m} r_m\right) h_i(x_1)\right) + \overline{\lambda}(x_1 - \overline{T}_a) \tag{8}$$

$$g(x) = -\frac{\Delta g}{2\overline{F}} + \frac{\overline{R} x_1}{2\overline{F}} \ln(Q) - \frac{x_5 x_2}{\overline{A}} \tag{9}$$

$$h(x) = \frac{\overline{k}_1 \overline{\mu}_f + \overline{k}_2}{1 + e^{\frac{x_1 - \overline{k}_3}{\overline{k}_4}}} \left(e^{\frac{\overline{k}_5 x_5}{\overline{A}}} - 1\right) \frac{1}{\overline{k}_0} \tag{10}$$

In particular, function f includes both the enthalpy balance and the heat losses of equation (1), function g represent the voltage expression in (2), and h is the gain of the degradation rate in (7). In h the simplification $\overline{\mu}_f = 1$ is made based on typical operating conditions of the cell. In practical scenarios, efforts are made to keep μ_f at high values to ensure that the cell operates at peak efficiency. As a result, setting $\overline{\mu}_f = 1$ is a conservative approximation that simplifies the model while capturing the behavior of a cell functioning under near-optimal conditions.

This leads us to the following state space formulation:

$$\dot{x} = \mathcal{F}(x,u) = \begin{cases} \dot{x}_1 = \dfrac{1}{\overline{c}_p}\left(f(x) - g(x)x_5\right) \\ \dot{x}_2 = h(x)x_2 \\ \dot{x}_3 = -\dfrac{1}{\overline{\tau}_{x_3}} x_3 + \dfrac{1}{\overline{\tau}_{x_3}} u_1 \\ \dot{x}_4 = -\dfrac{1}{\overline{\tau}_{x_4}} x_4 + \dfrac{1}{\overline{\tau}_{x_4}} u_2 \\ \dot{x}_5 = -\dfrac{1}{\overline{\tau}_{x_5}} x_5 + \dfrac{1}{\overline{\tau}_{x_5}} u_3 \end{cases} \tag{11}$$

This representation merges the cell dynamics with the voltage degradation, enabling simultaneous optimization of both real-time performance and long term deterioration of the system.

B. Control Problem Formulation

To implement the proposed Degradation-Conscious Nonlinear Model Predictive Control (DC-nMPC) strategy, we utilized the extended state-space model introduced in (11). The choice of a nMPC formulation is justified by its capability to handle nonlinearities and to include both input and state constraints, ensuring that control actions remain within operational limits.

The continuous-time model is internally discretized using a standard direct method, with zero-order hold (ZOH). From this point on, the subscript k will denote the discrete time step, applying to the state, inputs, and functions.

The nMPC control problem is defined as follows:

$$\min_{x,u} \quad \sum_{k=0}^{N-1} \left(J_{0,k} + \|u_k\|_R^2\right) \tag{12}$$

$$\text{subject to} \quad x_{k+1} = \mathcal{F}_k(x_k, u_k) \tag{13}$$

$$\overline{x}_{\min} \le x_k \le \overline{x}_{\max} \tag{14}$$

$$\overline{u}_{\min} \le u_k \le \overline{u}_{\max} \tag{15}$$

$$\overline{\Delta u}_{\min} \le u_{k+1} - u_k \le \overline{\Delta u}_{\max} \tag{16}$$

$$h_k(x_{1,k}, u_k)\, x_{2,k} \le \dot{\overline{R}}_{a,\max} \tag{17}$$

The cost function in (12) consists of two main terms. $J_{0,k}$ is responsible for reference tracking and degradation rate minimization and it is defined as follows:

$$J_{0,k} = Q_1(x_1 - T_{\text{ref},k})^2 + Q_2(g(x)x_5 - P_{\text{ref},k})^2 + Q_3(h(x)x_2 - \dot{R}_{a,\text{ref}})^2 \tag{18}$$

The first two terms in $J_{0,k}$ manage the cell's temperature and power tracking by penalizing deviations from their respective reference values at time k, namely $T_{\text{ref},k}$ and $P_{\text{ref},k}$. The last term manages the real time minimization of the degradation rate, to do so $\dot{R}_{a,\text{ref}} = 0$ is kept constant. Here, Q_i represent the weights applied to each term to prioritize the tracking objectives and degradation rate minimization.

The second term in (12) accounts for input regulation by penalizing deviations in the control input, ensuring that manipulated variables stay within desired bounds. In our formulation, R represents the weighting factor for the inputs, balancing control effort and system performance. Additionally, the slack variables for constraint violation are managed internally by the controller and are automatically included when necessary, ensuring constraint feasibility without requiring explicit user definition.

Looking at the constraints, (13), represents the state evolution equation, as detailed in (11). It describes how the system's state evolves over time as a function of the current state and control inputs. The constraints in (14) to (16) are derived from the physical and operational limits of the system, governing the admissible ranges for temperature and electric power output. These constraints are based on physical limits, such as the maximum allowable current I and the opening time of inlet valves, which define the feasible operating conditions of the cell.

Finally, since the objective of minimizing degradation is inversely related to the cell's operation (with degradation always positive and reaching zero only when the system is off), (17) introduces a constraint on the maximum allowable degradation rate, namely $\dot{\overline{R}}_{a,\max}$. This intervention is essential to mitigate the degradation effects, particularly during periods of high electric power demand.

IV. Simulation Results

The simulations have been performed in MATLAB Simulink environment. In Table I, we present the specifications of the overall tracking problem alongside the corresponding constraints. The main objective of the simulation is to achieve the following goals: provide the required power

profile, stabilize the temperature around a constant value while keeping it within operational limits, and minimize the degradation rate while restricting its maximum value.

TABLE I

REFERENCE VALUES AND I/O CONSTRAINTS

Reference Tracking	
Objective	**Details**
Temperature Tracking	T_{ref}: 1100 K, constant
Power Tracking	P_{ref}: Square Wave 7-17 W, 10 min cycle
Degradation Minimization	$\dot{R}_{a,\text{ref}}$: 0%/h, constant

Input and Output Constraints for SOFC System	
Description	**Constraint/Details**
Temperature x_1	$973\,\text{K} \leq T \leq 1133\,\text{K}$
Degradation rate $\dot{x}_2$	$h(x)x_2 \leq 0.45\%/\text{h}$[1]
Current u_1	$0\,\text{A} \leq I \leq 30\,\text{A}$, Max Rate: 5 A/min
Fuel input u_2	$0 \leq u_2 \leq 5 \times 10^{-4}$ mol/s,
	Max Rate[2]: 10% /min]
Air input u_3	$0 \leq u_3 \leq 3 \times 10^{-3}$ mol/s,
	Max Rate[2]: 10% /min

Two additional constraints, not explicitly in (12)-(17) are are the fuel utilization $\mu_f \in (0.5; 0.95)$, and air utilization $\mu_a \in (0; 0.8)$, chosen to reflect typical SOFC operation.

To evaluate the results, we tested the degradation-conscious implementation against a nMPC controller, which does not incorporate a degradation model, which assumes a constant $\overline{R}_a$ equal to the initial value in the DC-nMPC configuration. The parametrization of the two controllers is reported in Table II.

TABLE II

CONTROLLERS MAIN PROPERTIES

Property	**DC-nMPC**	**nMPC**
Sampling Time	10 s	10 s
Moving Horizon	30 steps	30 steps
Degradation Model	Yes	No, constant $\overline{R}_a$
Weight Q	diag(50, 500, 150)	diag(50, 500, 0)
Weight R	diag(1, 1, 1)	diag(1, 1, 1)

For a fair comparison, we kept the same parametrization, except for the last entry of the weighting matrix Q, which represents degradation minimization and is omitted in standard nMPC. While the dynamic model (1) and the experimental degradation model (7) are based on different SOFCs, we used the experimental value, which reflects slow degradation typically around 1-2%, over thousands of hours. This approach ensures the simulation remains realistic by accurately accounting for the gradual, minimal degradation over time. The main results are shown in Figure 2.

Starting from the temperature tracking, we see that the DC-nMPC keeps an overall higher temperature throughout the entire simulation with respect to the other controller. This

[1]The rate of change of voltage degradation is expressed in %/h of its nominal value (i.e., its value at the start of the simulation)

[2]Maximum ramp rates indicate a 10% change of the total valve opening, meaning it takes 10 minutes to go from fully closed to fully open.

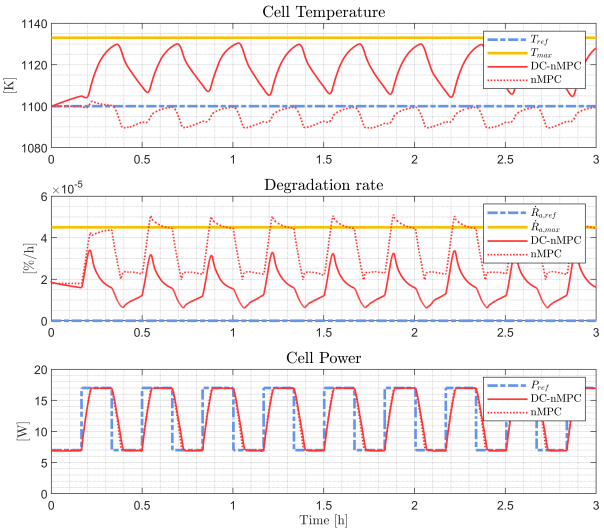

Fig. 2. Simulation results: cell temperature, voltage degradation rate and cell power

is due to the shape of our the voltage degradation function (7), which is inversely proportional to the cell temperature.

The power tracking results show that both controllers effectively follow the power profile.

The degradation rate is effectively bounded by the DC-nMPC, while the constraint is not included in the other controller. Moreover we see that throughout the entire simulation, irrespective of the power demand, the DC-nMPC seeks for a configuration in which the degradation rate is kept as low as possible. This indicates that the controller has identified an operating point that allows for precise power tracking while minimizing degradation compared to the other controller. This is even more evident when looking at the cumulated effect of these control choices, as we mentioned before, degradation manifests over thousands of hours of operation. By extending the shown 3-hour test to a total of 50 hours, the cumulative effect of these control choices reduced degradation from the standard 0.105% to 0.045%, as shown in Figure 3.

Last, although a single parametrization, as the one in in Table II, might not show the full picture, it provides a valuable comparison between the two strategies. In general we noticed that the DC-nMPC required longer horizons in order to converge to a stable configuration. This is primarily due to the fact that degradation depends on a relatively fast input, namely the current I, as well as on the cell temperature, which is instead a slow state of the system. As a result, guiding the system within the acceptable range of solutions required the controller to consider the effects of its decisions over a much longer horizon than the standard approach. Nevertheless, the DC-nMPC controller showed an overall improved management of cell degradation, both by limiting and by minimising its real-time value, and by making the controller aware of the long-term drift in R_a.

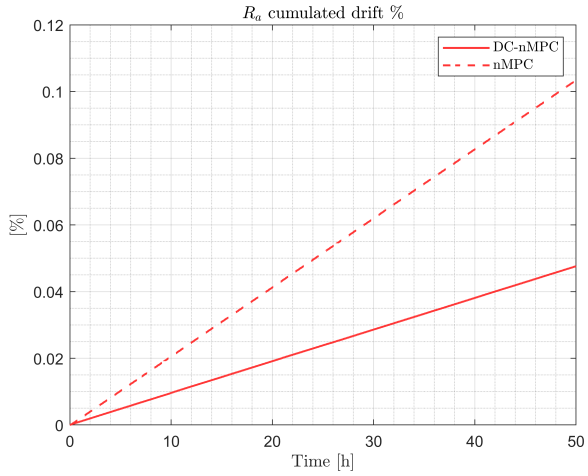

Fig. 3. Cumulate drift on the area specific resistance R_a due to voltage degradation, expressed as percentage of the nominal value.

V. Conclusion

In conclusion, this study highlights the importance of advanced control strategies to increase the resilience of Solid Oxide Fuel Cells (SOFCs) to long-term degradation effects while maintaining adequate dynamic performance. This capability is essential for the widespread adoption of this technology in the marine industry, particularly in the context of the sector's de-carbonisation process.

The proposed approach, Degradation-Conscious Nonlinear Model Predictive Control (DC-nMPC), is based on an extended SOFC system model that considers both cell dynamics and the degradation of its ohmic resistance due to operational factors. The results show that this method effectively addresses the challenges of ensuring dynamic performance while reducing cell voltage degradation.

Simulation results show that effective management of the cell degradation rate is achievable, but at the cost of increased overall computational complexity and potentially suboptimal dynamic performance.

Future work will incorporate performance analysis, including stability guarantees, and a sensitivity analysis of design parameters. Additionally, by incorporating knowledge of degradation evolution, the approach could be extended to use a Remaining Useful Life (RUL) metric, enabling the selection of a time-to-failure or expected lifetime of the equipment as a control objective. Such advancements could enable a more proactive management of operational lifetimes and further support the deployment of these technologies across the maritime sector and beyond.

References

[1] H. Yokokawa, H. Tu, B. Iwanschitz, and A. Mai, "Fundamental mechanisms limiting solid oxide fuel cell durability," *Journal of Power Sources*, vol. 182, no. 2, pp. 400–412, 2008.

[2] S. Zarabi Golkhatmi, M. I. Asghar, and P. D. Lund, "A review on solid oxide fuel cell durability: Latest progress, mechanisms, and study tools," *Renewable and Sustainable Energy Reviews*, vol. 161, p. 112 339, 2022.

[3] P. Aguiar, C. Adjiman, and N. Brandon, "Anode-supported intermediate-temperature direct internal reforming solid oxide fuel cell: Ii. model-based dynamic performance and control," *Journal of Power Sources*, vol. 147, no. 1, pp. 136–147, 2005.

[4] A. Y. Sendjaja and V. Kariwala, "Decentralized control of solid oxide fuel cells," *IEEE Transactions on Industrial Informatics*, vol. 7, pp. 163–170, 2 May 2011.

[5] B. Yang, Y. Li, J. Li, *et al.*, "Comprehensive summary of solid oxide fuel cell control: A state-of-the-art review," *Protection and Control of Modern Power Systems*, vol. 7, p. 36, 2022.

[6] X. Zhang, S. Chan, H. Ho, J. Li, G. Li, and Z. Feng, "Nonlinear model predictive control based on the moving horizon state estimation for the solid oxide fuel cell," *International Journal of Hydrogen Energy*, vol. 33, no. 9, pp. 2355–2366, 2008.

[7] J. Li, T. Yu, and B. Yang, "A data-driven output voltage control of solid oxide fuel cell using multi-agent deep reinforcement learning," *Applied Energy*, vol. 298, p. 117 541, 2021.

[8] A. Sorce, A. Greco, L. Magistri, and P. Costamagna, "Fdi oriented modeling of an experimental sofc system, model validation and simulation of faulty states," *Applied Energy*, vol. 136, pp. 894–908, 2014.

[9] B. Dolenc, P. Boškoski, M. Stepančič, A. Pohjoranta, and Juričić, "State of health estimation and remaining useful life prediction of solid oxide fuel cell stack," *Energy Conversion and Management*, vol. 148, pp. 993–1002, 2017.

[10] T. Escobet, J. Quevedo, V. Puig, and F. Nejjari, "Combining health monitoring and control," in *Diagnostics and Prognostics of Engineering Systems: Methods and Techniques*, IGI Global, 2012, pp. 230–255.

[11] A. Goshtasbi and T. Ersal, "Degradation-conscious control for enhanced lifetime of automotive polymer electrolyte membrane fuel cells," *Journal of Power Sources*, vol. 457, p. 227 996, 2020.

[12] L. van Biert, P. S. Castillo, A. Haseltalab, and R. R. Negenborn, "A reduced-order model of a solid oxide fuel cell stack for model predictive control," in *Proceedings of the International Ship Control Systems Symposium*, 2022.

[13] V. Zaccaria, D. Tucker, and A. Traverso, "A distributed real-time model of degradation in a solid oxide fuel cell, part i: Model characterization," *Journal of Power Sources*, vol. 311, pp. 175–181, 2016.

[14] L. van Biert, M. Godjevac, K. Visser, and P. Aravind, "Dynamic modelling of a direct internal reforming solid oxide fuel cell stack based on single cell experiments," *Applied Energy*, vol. 250, pp. 976–990, 2019.

[15] P. J. Linstrom, W. G. Mallard, N. I. of Standards, and T. (U.S.), *Nist chemistry webbook*, Aug. 1997 release, 1997. [Online]. Available: `https://webbook.nist.gov/chemistry/`.

[16] C. H. Shomate, "A method for evaluating and correlating thermodynamic data," *The Journal of Physical Chemistry*, vol. 58, no. 4, pp. 368–372, 1954.

[17] Z. Lyu, H. Li, M. Han, Z. Sun, and K. Sun, "Performance degradation analysis of solid oxide fuel cells using dynamic electrochemical impedance spectroscopy," *Journal of Power Sources*, vol. 538, p. 231 569, 2022.